

# Analysis and Simulation of Automotive Interleaved Buck Converter

Mohamed. A. Shrud, Ahmad H. Kharaz, Ahmed. S. Ashur, Ahmed Faris and Mustafa Benamar

**Abstract**—This paper will focus on modeling, analysis and simulation of a 42V/14V dc/dc converter based architecture. This architecture is considered to be technically a viable solution for automotive dual-voltage power system for passenger car in the near further. An interleaved dc/dc converter system is chosen for the automotive converter topology due to its advantages regarding filter reduction, dynamic response, and power management. Presented herein, is a model based on one kilowatt interleaved six-phase buck converter designed to operate in a Discontinuous Conduction Mode (DCM). The control strategy of the converter is based on a voltage-mode-controlled Pulse Width Modulation (PWM) with a Proportional-Integral-Derivative (PID). The effectiveness of the interleaved step-down converter is verified through simulation results using control-oriented simulator, MatLab/Simulink.

**Keywords**—Automotive, dc-to-dc power modules, design, interleaved, Matlab/Simulink and PID control.

## I. INTRODUCTION

A switching converter is an electronic power system which transforms an input voltage level into another for a given load by switching action of semiconductor devices. A high power efficient dc-dc converter is strongly desired and has found widespread applications. Examples include aerospace [1], sea and undersea vehicles [2], electric vehicles (EV), Hybrid Electric Vehicle (HEV) [3], portable electronic devices like pagers [4], and microprocessor voltage regulation [5].

In dual-voltage vehicular electrical systems, the dc-to-dc converter is required to step-down the high-voltage to provide back up compatibility for the existing low-power devices such as lamps, small electric motors, control units and key-off load (clock, security system). A schematic of the 42V/14V dc-to-dc converter architecture is shown in Fig.1, with the possibility of either single or a dual battery (12V and 36V). The aim of the 42V/14V architecture of Fig.1 is to reduce the cost, weight and packaging space created by the additional 12V energy storage battery. Ideally, the power management system should be smart enough to manage the key-off loads from depleting the high voltage battery to the point that the car cannot be started

[6]. The philosophy behind dual battery system architecture is that the starting function should be isolated from the storage function required for the key-off loads [7].

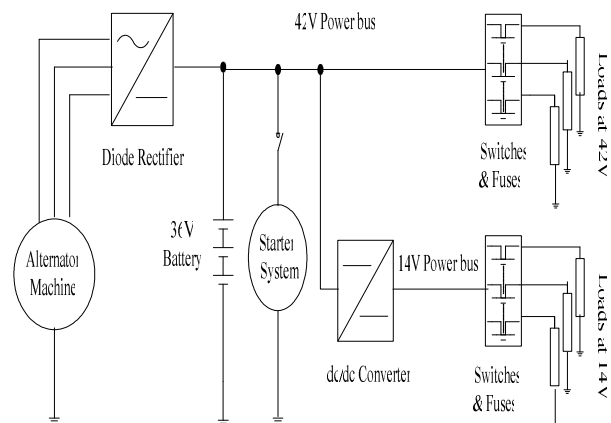


Fig. 1 The 42V/14V system architecture

For automotive application where volume, weight, and cost are particularly important, the preferred choice is the single battery 42V/14V system architecture with centralized system structure. Furthermore, the removal of the 12V battery does not alter the dynamics of operation of the power converter. But the power from the converter must cover the power requirement of all the 14V power loads (approximately 1kW) under the worst-case scenario.

In addition, the non-isolated dc/dc converter topology is the most appropriate architecture because isolation between 42V and 14V buses is not required in automotive power net and has the advantage over the transformer-isolation types in terms of the easy-to-design circuit configuration, low volume, weight and cost.

An important portion of the integrated circuit industries such as (Linear Technology Corporation and Texas Instrument) are focusing their efforts in developing more efficient and reliable step-down (Buck) converters. In academic, research studies into analysis, modeling and simulation of 42V/14V dc/dc converters have made progress in various disciplines, including thermal, electrical and mechanical analysis.

A strategic methodology to the design power of electronic equipments is presented in [8]. Investigation of computer-aided design (CAD) tool to calculate the number of phases to

M. A. Shrud is with High Institute of Electronic Professions, Tripoli, Libya (mshrud@hotmail.com).

A. H. Kharaz is with the School of Technology, University of Derby, Derby, UK (e-mail: a.kharaz@derby.ac.uk).

A. S. Ashur is with Alfateh University, Tripoli, Libya (e-mail: a.ashur@hotmail.co.uk).

A. Faris is with the University of Derby, Derby, UK (e-mail: a.faris@derby.ac.uk).

M. Benamar is with Libyan Civil Aviation, Air Navigation Department, Tripoli-Libya (e-mail: benamar11@hotmail.com).

optimize cost, size, and weight is offered in [9]. The power losses in a 500W converter as a function of the number of phases are explained in [10]. The effect of number of cells on the passive component using software tool called PExprt is carried out in [11]. A comparison between multi-phase converters with a conventional single-switch buck converter is carried out in [12]. State of the art engineering for multi-phase dc/dc converter may range from three, four to five paralleled buck stages [9,12] or even as many as 16 and 32 phases [13,14].

Taking one step further in this direction, a model based on one kilowatt interleaved six-phase dc-to-dc buck converter designed to operate in a Discontinuous Conduction Mode (DCM) controlled by voltage-mode-controlled Pulse Width Modulation (PWM) with a Proportional Integral Derivative (PID) is presented. The effectiveness of the interleaved step-down converter system is verified through simulation results using control-oriented simulators, MatLab/Simulink.

## II. DC-TO-DC POWER MODULE

A single step-down converter system typically involve switching circuits composed of semiconductor switches such as, MOSFETs and diodes, along with passive elements such as inductors, capacitors, and resistors as shown in Fig. 2a. The main switching waveforms of the inductor voltage and current under steady-state conditions are sketched in figure 2b for Critical Discontinuous Conduction Mode (CDCM) and in figure 2c for Discontinuous Conduction Mode (DCM) of operation. The gating signal,  $q(t) \in [0, 1]$  is the control variable that models the MOSFET switch. When the value of the control variable  $q(t) = 1$ , the MOSFET is *ON*, and zero when the MOSFET is *OFF*.

Assuming that the converter is operating under CDCM of operation as shown in Fig 2(b), the operation of this circuit can be explained as follows; the operation of this circuit can be explained as follows;

- During the turn-on period of the high-side switch, the input voltage is connected to the inductor and the diode is *OFF*. According to Lenz's law, the voltage across a coil is equal to the instantaneous rate of change in current multiplied by the self inductance of the coil. Therefore, the mathematic equations for this interval is given by:

$$(1) V_L = L \times \frac{\Delta I}{\Delta t}$$

Rearranging equation (1) becomes;

$$\Delta t = \frac{V_L}{L} \times \Delta t \quad (2)$$

The maximum inductor current is given by;

$$I_{\max} = \frac{V_L}{L} \times D \times T \quad (3)$$

Where:  $T = 1/f_s$ ,  $f_s$  is the converter switching frequency and  $D$  is switching duty cycle for the MOSFET switch, defined by  $t_{on}/T$ . Equation 3 can be rewritten in the form of,

$$I_{\max} = \left( \frac{(V_i - V_o)}{f_s L} \right) \quad (4)$$

Upon inspection of figure 2(b),  $I_{\max}$  is twice the phase averaged current, therefore, the average value of inductor current is described by the following relationship:

$$(5) I_{avg} = \frac{(V_i - V_o) V_i D^2}{2 L f_s V_o}$$

This equation states that, the output current is characterized by the bus voltages, inductance and the switching frequency. At the end of turn-on period, as soon as the switch is turned *OFF* and the diode is *ON* to keeps inductor current flowing. The rate of fall in the inductor current during the freewheeling period is;

$$\frac{\Delta I}{\Delta t} = -\frac{V_o}{L} \quad (6)$$

The above procedure could be repeated easily during the *OFF* interval,  $(1-D)T$  to determine the same state variable equation of the average value of inductor current  $I_{avg}$ .

As can be seen from Fig 2(c), the value of the inductance needed to ensure that the converter remains in Discontinuous Conduction Mode (DCM) of operation i.e. the inductor current is zero during part of the switching period and both semiconductor devices are *OFF* during some part of each cycle must be less than  $L_{critical}$ , which can be determined as follow.

$$L_{critical} = \frac{V_i D^2}{2 f_s I_{\max}} \times \frac{V_i - V_o}{V_o} \quad (7)$$

Where:  $L < L_{critical}$

However, the standard dc/dc converter with single structure is not feasible due to the low voltage (14V) high current (71A), and high operating temperature characteristics of the converter specification. Therefore, most of the power stage of the converter would have to be built in parallel for practical implementation. A common approach in technical literature and industry practice is to use interleaved multi-phase technique instead of a single larger converter [15,16]. This approach is an attractive solution and its benefits will be discussed in the next section.

### III. MULTIPHASE SWITCHING OF DC-TO-DC CONVERTERS

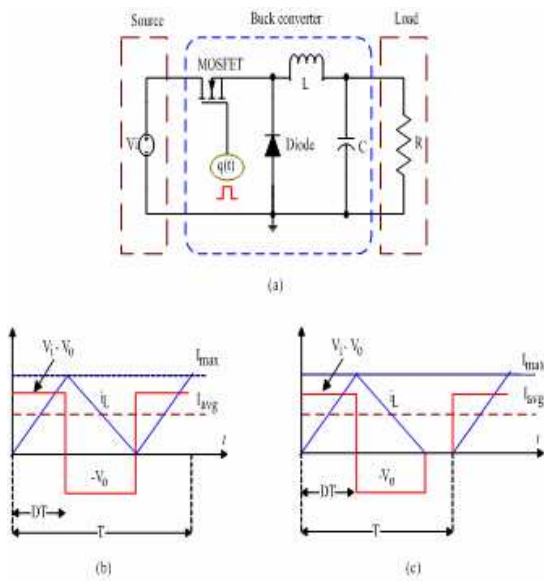


Fig. 2 (a) A single-buck converter topology, (b) Typical CDCM excitation and (c) A DCM excitation current waveforms

To realize power conversion by a simple system configuration, a multi-cells buck converter topology designed for DCM of operation is employed. Fig. 3 shows the developed Simulink diagram of six-cells interleaved buck converter with PID Controller.

The six-cell interleaved buck converter is connected in parallel to a common output capacitor and sharing a common load with associated control system. The low-voltage side is connected to the 14V automotive electrical loads while the high-voltage side to the on-board power generator (alternator) with nominal input voltage of 42V, and range between 30V and 50V during normal operation.

In this interleaved six-cell dc/dc converter architecture, the cells are switched with the same duty ratio, but with a relative phase shift or time interleaved of  $60^\circ$  introduced between each cell in order to reduce the magnitude of the output ripple at the output port of the converter. The overall output current is achieved by the summation of the output currents of the cells. With the phase shift of  $60^\circ$ , the output of the converter is found to be continuous.

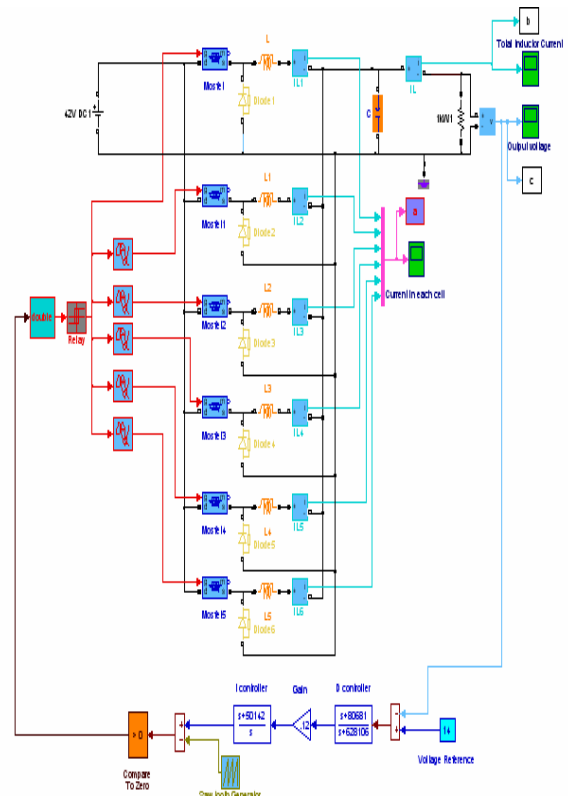


Fig. 3 Simulink implementation of the interleaved six phase buck converter circuit with PID controller

The ripple reduction helps to reduce the filtration requirements needed to contain any EMI the converter produces and thereby decrease the constraints on the electronics components connected to the low-voltage bus. Furthermore, due to the equal sharing of the load current between cells, the stress on the semiconductor switches is reduced and thereby reliability is improved. Another advantage is the ability to operate the converter when a failure occurs in one cell as well as the possibility to add new cells to the converter with minimum effort.

To design this converter, the following automotive specifications for dual-voltage automotive electrical systems must be fulfilled and are tabulated in table 1[8, 9, 17]. The specifications of the converter should meet the demand of the 14V electrical loads of 71A, operating temperature range  $-40^\circ\text{C}$  to  $90^\circ\text{C}$  and the tight EMI requirements to prevent the converter from interfering with other equipment in the car. Adding to this, the converter should provide high performance and high reliability at low cost.

TABLE I  
DESIGN SPECIFICATIONS FOR A POWER CONVERTER IN A DUAL-VOLTAGE  
AUTOMOTIVE ELECTRICAL SYSTEM

Description	Parameter	Value
Operation input voltage	$V_i$	30V<42V<50V
Operation output voltage	$V_o$	11V<14V<16V
Power rating	$P_o$	1kW
Operation temperature range	$T$	-40C<T<90C
Output ripple voltage	$\Delta V_o$	300mV
Output ripple current	$\Delta I_o$	1A

TABLE II  
CAPACITOR VALUE VERSUS VOLTAGE /CURRENT RIPPLE

Capacitor value	Output voltage ripple	Output current ripple
100 $\mu$ F	6mV	30mA
150 $\mu$ F	4mV	20mA
200 $\mu$ F	3mV	16mA
250 $\mu$ F	2.5mV	12mA
300 $\mu$ F	2mv	10mA
350 $\mu$ F	1.5mV	9mA
400 $\mu$ F	1mV	7mA

#### IV. COMPONENT SELECTION

For low voltage/high current power converter, the usage of MOSFETs switching devices with low on-resistance is required for more efficient and practical power conversion. The inductors and capacitors play important roles in the design of the power converter. Inductor is an energy storage element while the capacitor is the main buffer for absorbing the ripple current generated by the switching action of the power stage. The switching frequency of the power electronics used in automotive industry ranges from 82 kHz to 200 kHz with 100 kHz as a typical value used for most operation of dc/dc converters.

Based on the switching frequency, input/output voltages and the duty ratio, the inductance value to guarantee that the converter cells would run in the discontinuous conduction mode DCM over the entire operating range can be calculated using the following equation

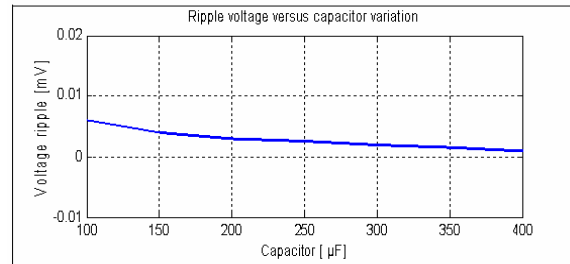
$$L_{critical} = -\frac{V_i D^2}{2f_s I_{max}} \times \frac{V_i - V_o}{V_o} \quad (8)$$

Since this is a six-phase interleaving converter, the power stage inductance of each phase is therefore equal to 2.4 $\mu$ H. The output capacitor is another important element, which may reduce the system cost in multi-phase converter system and is needed to keep the output voltage ripple  $\Delta V_o$  within allowable output voltage range. To meet these constraints of the design specifications, the capacitor value does not necessarily need to be very large to smooth the output voltage. Table 2 shows the capacitor variation from 100 $\mu$ F to 400 $\mu$ F along with the value of voltage/current ripple while figure 4 shows the plot of output ripple voltage versus capacitor value from the simulation analysis obtained. To meet the constraint of the design requirements concerning the voltage ripple of the converter system, a capacitor value of 300 $\mu$ F is sufficient.

#### V. CONTROL DESIGN STRATEGIES

Feedback is used in control systems to change the dynamic behavior of the system, whether mechanical, electrical, or biological, and to maintain their stability. The control strategy of the proposed converter is based on a voltage-mode-controlled Pulse Width Modulation (PWM)

Fig. 4 Ripple voltage versus capacitor values



with a Proportional-Integral-Derivative (PID) which takes its control signal from the output voltage of the switching converter instead of current-mode (or current-injected) PWM, which utilizes both the output voltage information and the current information from the inductor to determine the desired duty cycle. A Simulink model for the internal structure of the PID used to control the converter is shown in Fig. 5.

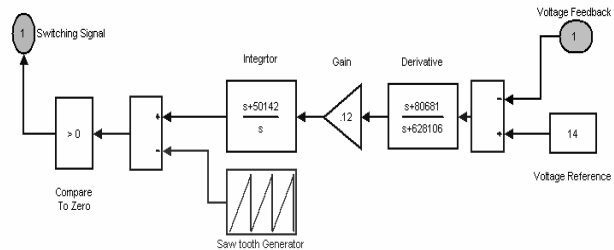


Fig. 5 A PID controller represented by a Simulink block diagram

The aim is to regulate the output voltage of the converter  $V_o$  across the load resistance  $R_L$  to match a precise stable reference voltage  $V_{ref}$ . This is achieved by subtracting the desired reference voltage  $V_{ref}$  from the sensed output Voltage  $V_o$  of the converter. The voltage-error thus obtained is passed through a PID controller to obtain the desired signal. The function of the PID controller is to take the input signal, compute its derivative and integral, and then compute the output as a combination of input signal, derivative and integral. The individual effects of P, I, and D tuning on the closed-loop response are summarized in table 3[18].

TABLE III  
EFFECT OF INDEPENDENT P, I, AND D DURING THE TUNING PROCESS

Closed-Loop response	Rise time	Overshot	Settling time	Steady state error	Stability
Increasing $P$	Decrease	Increase	Small increase	Decrease	Degrade
Increasing $I$	Small decrease	Increase	Increase	Large decrease	Degrade
Increasing $D$	Small decrease	Decrease	Decrease	Minor decrease	Improve

The desired output generated signal of the PID controller is fed to the Pulse Width Modulation (PWM) unit, where it is compared with a constant frequency saw tooth voltage  $V_{pwm}$ . The frequency of saw tooth voltage is the switching frequency  $f_s$  of the converter which is 100 kHz. The output signal from the PWM is the switching control signal, which represents a sequence of pulses that drives the semiconductor switch, as shown in fig 6.

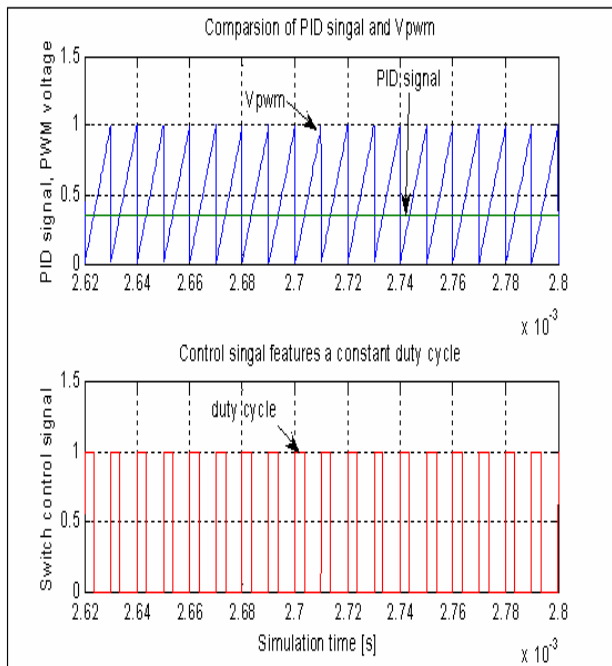


Fig. 6 Implementation of Pulse Width Modulation in Simulink.

The proposed converter necessitates a phase-shift of  $60^\circ$  between the cells to generate the six-switching control signal which are used to drive the six active MOSFET switching devices of the converter system. Figure 7 and 8 shows the implementation of the six-phase interleaving circuit in Simulink and the six phase control signal waveforms respectively.

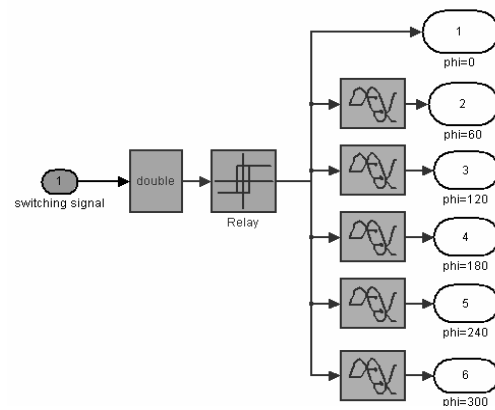


Fig.7 Six phases of interleaving in Simulink

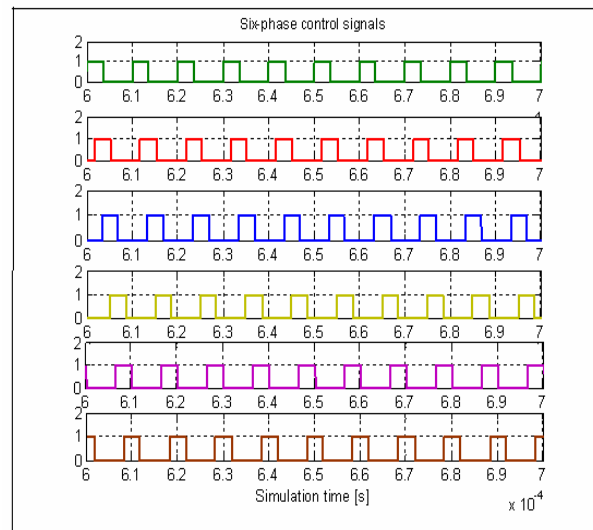


Fig. 8 Six-phase control signals in Simulink

## VI. MATLAB/SIMULINK SIMULATIONS AND RESULTS

The ability to model and simulate engineering design of a complete power electronic converter system is essential before proceeding to the engineering experimental phase. Hence, simulations are important for design validations and cost-effectiveness as the power-conversion product development. The complete model of the Simulink implementation of the internal structure of the interleaved six-phase buck converter system is shown in Fig.9. The converter system is divided into three main parts; the six-cell buck converter, the voltage-mode-controlled PWM with a PID controller and the phase shift interleaving circuit. The multi-phase converter has been simulated to obtain the necessary waveforms that describe converter system operation under steady-state and transient conditions, using the design parameters tabulated in table 4.

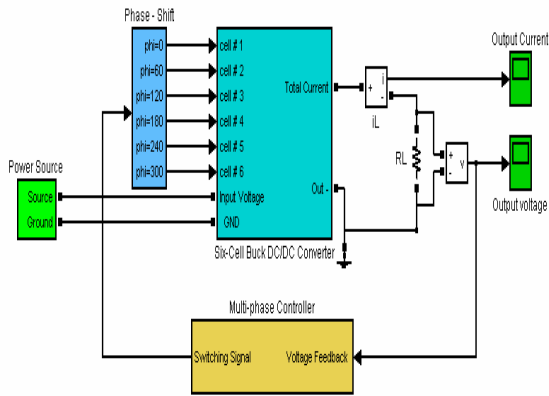


Fig. 9 Simulink schematic diagram illustrating the implementation of interleaved six-phase buck converter circuit with a PID controller

TABLE IV  
THE CONVERTER MAIN CIRCUIT PARAMETERS

Parameter Name	Symbol	Value	Units
Input voltage	$V_i$	42	V
Output voltage	$V_o$	14	V
Number of phases	N	6	-
Inductor value	L	2.4	$\mu\text{H}$
Capacitor value	C	300	$\mu\text{F}$
Load resistance	RL	0.196	$\Omega$
Switching frequency	fs	100	kHz

#### A. Ripple Cancellation

The first step in the analysis of the multi-phase interleaved converter system is to investigate the effectiveness of ripple-cancellation related to the variation of current and voltage as a function of the number of cells. Table 5 shows a summary of results generated by Simulink during the simulation of four interleaved converter with the same control design strategies.

TABLE V  
OUTPUT VOLTAGE AND CURRENT RIPPLES VERSUS THE NUMBER OF CELLS

Number of phases	4	6	8	10
Output voltage ripple	8.7mV	2 mV	1.1mV	0.5mV
Output current ripple	45mA	9mA	6mA	3.2mA

From the results it can be observed that the converter achieves a very good current and voltage ripple cancellation for four-cells and above. Though, eight or ten-cells produce a better ripple-cancellation, however, the cost outweigh the gains in accuracy. The results also show that the EMI filter is not needed to reduce the peak to peak voltage ripple on the 14V terminal. This may lead to the elimination or redesign of the protection circuitry connected to the 14V bus. It also can be seen from Fig 10 that the ripple of the output voltage and the total inductor current of the power converter system are better than the desired specified limits indicated in table 1.

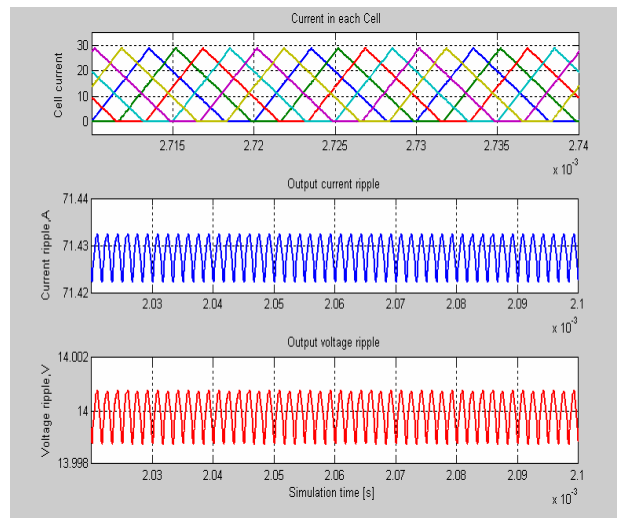


Fig. 10 Current and voltage output ripples

Fig.11 shows the steady-state waveforms of the individual cell currents, the total output inductor current and the output voltage. The simulated results show that the curves of the individual cell currents are balanced and the time interleaved of the cells is apparent from the relative time delay of each cell's inductor current. The inductor current in each cell rises to 30A during each switching period and goes through an interval in the discontinuous conduction mode.

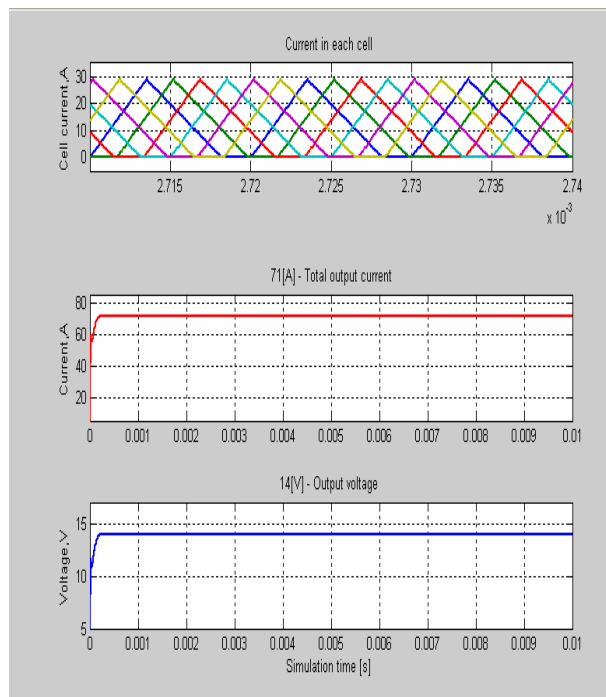


Fig .11 Top trace is the individual cell currents then total output current and bottom trace is the output voltage of the converter system

The sum of the individual cell currents result in a total current of 71A with a ripple current of around 9mA which is less than the individual cell ripple current. The simulated results indicate that, the operation of the power converter system is stable and accurate. The converter is able to respond and produce the desired stable output voltage and deliver the required total output current to the load with very low ripple. As a result, no negative effect on the connected loads, such as small motors, lights and accessories.

#### B. Transient Simulation for Load Variation

The interleaved dc/dc buck converters are used as power source to resistive and dynamic loads (motors) in passenger car and these loads could be categorized into;

- Small motors (2 to 8A @12V).
- Very small motors ( less than 2A @12V )
- Lighting system: internal lights, external lights, head lights.
- ECU and Key-off loads.

The electrical loads demand varies and depends upon the weather and the driving conditions. A full load condition is rarely present for a prolonged period of time and most of the devices run at light loads (stand-by-mode) for most of the time. To study the effect of the load variation on the dynamic behavior of the converter system, the load at the output of the converter system is suddenly changed from 50% to 75% and to 100% and than back from 100% to 75% and 50% of the full load at time  $t=0.002$ ,  $0.004$  and  $0.006$ s respectively. The simulated results are shown in Fig. 12.

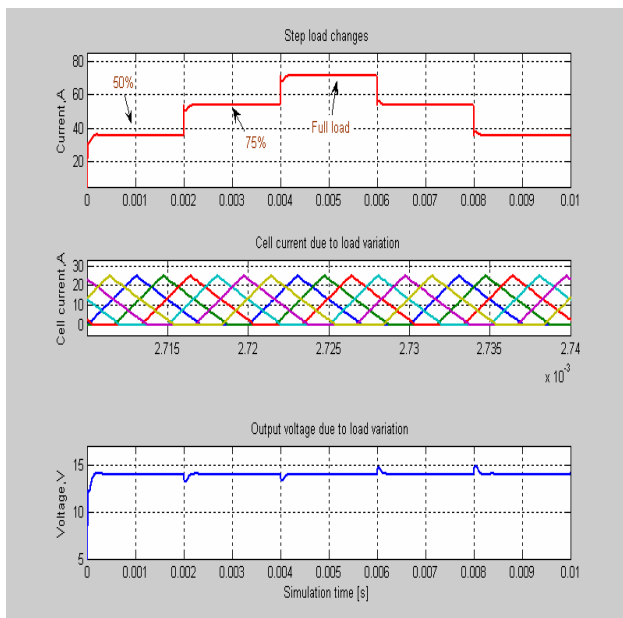


Fig. 12 Transient response of the output voltage to step change in load

It can be seen that the output voltage undershoot varies from 13.12V to 13.28V while the overshoot from 14.74V to 14.89V, when the load at the output of the converter system was suddenly changed from 50% to 75% and to full-load (1kW). The results show that the performance of the system is stable and well behaved under load variations (disturbances) and the output voltage remains within the desired specified limits presented earlier in table 1.

#### C. Input Voltage Variation

In real conditions, the alternator output voltage ranges from 30V to 50V during normal operation, with nominal voltage of 42V. To study this line of variation, a step change in the input voltage from 33V to 50V is applied to the model. Fig.13 shows a transient response of the output voltage behaviour waveform due to sudden changes in the input voltage of the power converter system.

At the beginning of the cycle, at time  $t=0.004$ s, the input voltage suddenly rises from nominal system voltage of 42V to 50V. The maximum output voltage (bottom trace) transient is 15.09V, but after a short period of time this error is leveled out in approximately 200ms with a maximum overshoot of 1.09V. At instant time of  $t=0.01$ s, when the input voltage suddenly reduces from 50V to 33V, the output maximum transient voltage is 11.704V. The settling time to return to 14V is approximately 0.4ms with maximum overshoot of 2.296V. Finally, at time  $t=0.016$ s, when the input voltage suddenly increases from, 33V to the nominal system voltage, the maximum output transient voltage is 5.85V. The settling time for this is approximately 0.4ms with a maximum overshoot of 1.85V. The simulation results illustrate that the converter system has a strong immunity against line voltage disturbances even with the 12V energy storage battery being absent.

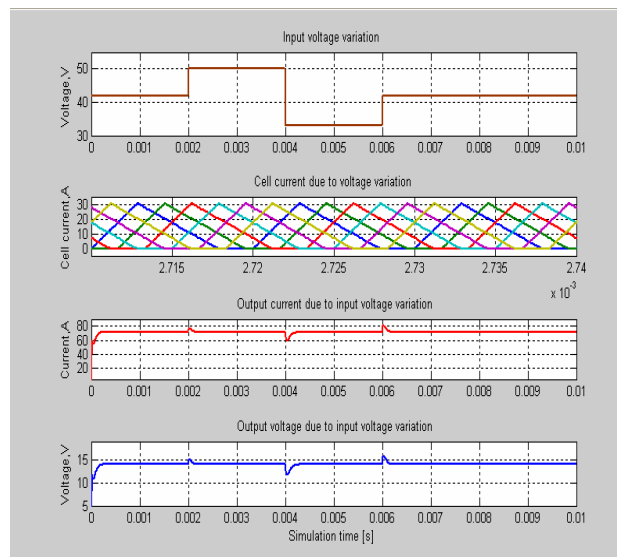


Fig. 13 Output voltage due to step line voltage disturbance.



#### D. Load and Supply Voltage Variations

The combinations of both the supply-voltage and load variations that occur in the converter system have been simulated and the outputs are presented in Fig.14.

It can be observed that the designed system has a low-sensitivity to the load and supply-voltage variations. These variations have only small influence on the output voltage and load current and still respect the specifications of the automotive standard. It can be concluded that from the results obtained the proposed converter can maintain the desired output voltage independently of load and supply-voltage variations. This may lead to the elimination or redesign of protection circuitry for electronics connected to the 14 V bus.

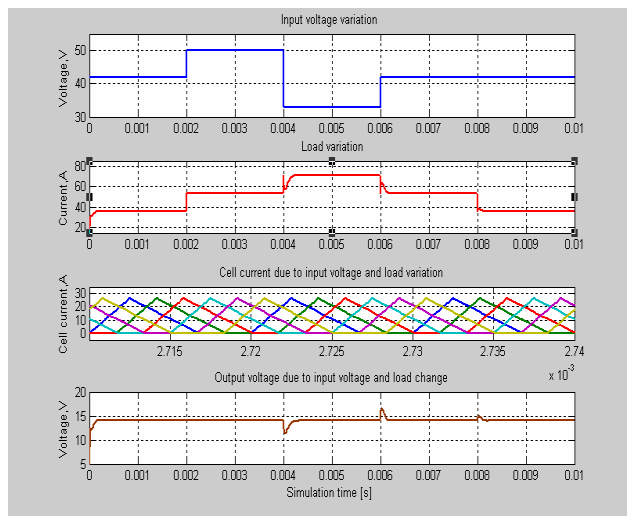


Fig. 14 Load current and output voltage due to under line voltage and load change disturbance

#### VII. CONCLUSION

In this paper, analysis, design and simulation of 42V/14V interleaved six-phase dc-to-dc buck converter system with one kilowatt output power was presented. This system is the heart of the dual-voltage architecture shown in figure1. Based on the simulation results, the performance of the dc-to-dc buck converter system provides a number of features that do not exist in today's electrical systems. Among these features is a well-regulated 14V bus even in the absence of a 12V storage battery. Therefore, no transient suppression is necessary at the 14V output. This improved transient response may lead to the elimination or redesign of protection circuitry for electronics connected to the 14V bus. Moreover, good stability, robustness, fast dynamic response and equal current distribution were achieved; at the same time the specification of the automotive standards were respected. Nevertheless, its application to a Voltage Regulator Module (VRM) is straightforward and it can be easily extended to cover other topologies.

#### ACKNOWLEDGMENT

The authors would like to thanks Mr. Salah Deen Kalifa, Director of Higher Institute of Electronic Professions, Libya for the friendship and overall support.

#### REFERENCES

- [1] A. Emadi, M Ehsani, and J.M.Miller., "Vehicular Electric Power Systems: Land, Sea, Air, and Space Vehicles", New York: Marcel Decker, (2003).
- [2] Claudio H. Rivetta, Ali Emadi, Geoffrey A. Williamson, Ranjit Jayabalan, and Babak Fahimi, "Analysis and Control of a buck DC-DC Converter Operating with Constant Power Load in Sea and Undersea Vehicles.", IEEE Transactions on Industry Applications, Vol.42, NO.2, March/April, (2006).
- [3] L.A.Khan, "DC-to-DC Converters for Electric and Hybrid Vehicles", Proceedings of IEEE Workshop on Power Electronics in Transportations, 1994 Record, pp.113-122, (1994).
- [4] Barry Arbetter, Robert Erickson, and Dragan Maksimovic, "DC-DC Converter Design for Battery -Operated Systems", Power Electronics Specialists Conference, PESC '95Record, 26th Annual IEEE, Vol.1, pp.103-109, Jun, (1995).
- [5] Angel Vladimirov Peterchev "Digital Pulse-Width Modulation Control in Power Electronic Circuits: Theory and Applications" Doctor of Philosophy in Engineering-Electrical Engineering and Computer Sciences, University of California, Berkeley, spring (2005).
- [6] J.M.Altes, E.G. Dolcet, and B.P. Solorzano. "Analysis of the Most Appropriate Electrical Architecture and Communication Bus for the New Dual Voltage 14/42v System", IECON-2002: Proceedings of the 2002 28th Annual Conference of the IEEE Industrial Electronics Society, Vol.1-4, pp. 1687-1692, (2002).
- [7] Ali Emadi, Sheldon S. Williamson, and Alireza Khaligh, "Power Electronics Intensive Solutions for Advanced Electric, Hybrid Electric, and Fuel Cell Vehicular Power Systems" IEEE Transactions on Power Electronics, Vol.21, NO.3, May, (2006).
- [8] L.Jourdan, J. L. Schanen, J.Roudet, M. Bensaeid, and K.Segueni, "Design methodology for non insulated DC-DC converter: application to 42 V-14 V Power-net," in Proc. IEEE Power Electron. Spec. Conf. (PESC'02), Vol. 4, pp. 1679-1684, (2002).
- [9] Timothy C. Neugebauer and David J. Perreault "Computer aided optimization of DC/DC converters for automotive applications," IEEE Transactions on Power Electronics, Vol.18., NO.3, May, (2003).
- [10] M.Gerber, J. A. Ferreira, I. W. Hofsaer, and N. Seliger, "Interleaving optimization in synchronous rectified DC/DC converters," in Proc. IEEE Power Electron. Spec. Conf. (PESC'04), pp. 4655-4661, (2004).
- [11] J. A. Oliver, P. Zumel, O. García, J. A. Cobos, and J. Uceda, "Passive component analysis in interleaved buck converters," in Proc. IEEE Appl. Power Electron. Conf. (APEC'04), Vol. 1, pp. 623-628, (2004).
- [12] A. Consoli, G. Scarcella, G. Giannetto, and A. Testa, "A multiphase DC/DC converter for automotive dual voltage power systems", Industry Applications Magazine, IEEE, Vol.10, Issue 6, pp. 35 - 42, Nov.-Dec, (2004).
- [13] O. Garcia, P. Zumel, A. de Castro, J. A. Cobos, and J. Uceda, "An automotive 16 phases DC/DC converter," in Proc. IEEE Power Electron. Spec. Conf. (PESC'04), Vol. 1, pp. 350-355, (2004).
- [14] Oscar García, Pablo Zumel, Angel de Castro, and José A. Cobos, "Automotive DC-DC Bidirectional Converter Made With Many Interleaved Buck Stages" IEEE Transactions On Power Electronics, Vol.21., NO.3, May (2006).
- [15] B. A. Miwa, D.M. Otten, M.E. Schlecht, "High efficiency power factor correction using interleaving techniques", Applied Power Electronics Conference and Exposition, pp 557-56, (1992).
- [16] "High-frequency multiphase controller," Tech. Rep. TPS40090, Texas Instrument Datasheet, Oct. (2003).
- [17] F. Z. Peng, F. Zhang, and Z. Quian, "A magnetic-less dc-dc converter for dual voltage automotive systems," IEEE Industry Applications, Vol.39, No.2, pp.511-518, Mar. /Apr. (2003).
- [18] Kiam Heong Ang, Gregory Chong, and Yun Li, "PID Control System Analysis, Design, and Technology", IEEE Transaction on Control Systems Technology, Vol.13, No. 4, July, (2005).